

New ways to improve the performance of near-room temperature photodetectors

J. PIOTROWSKI

VIGO Ltd

ul. Radiowa 3, 00-908 Warszawa, Poland

The major drawback of IR photodetectors is the need for cooling to suppress thermal generation of free carriers, which results in noise. New ways to improve the performance of infrared photodetectors that operate without cryogenical cooling are discussed in this article. Included is discussion of the optimum design of such devices, optical immersion of photodetectors to high refraction index, and the optical resonant cavity principle. The most promising way to reduce noise without cooling, however, is to suppress thermal generation by depleting the semiconductor in charge carriers, which is governed by Auger mechanism. Stationary depletion can be achieved by the use of exclusion, extraction and magnetoconcentration effects. The combination of various methods would eventually enable one to achieve near-background limited infrared photodetector (BLIP) performance without any cooling, whatsoever.

The ultimate signal-to-noise performance of semiconductor photodetectors is limited by statistical fluctuations of the thermal generation and recombination rates in the volume of photodetector material [1-2]. At high temperatures and in narrow gap semiconductors required for the middle and long wavelength photodetectors, both rates are determined by the

Auger processes [3-5]. High Auger generation and recombination rates make near-room temperature IR photodetectors very noisy. Cooling is very effective but rather impractical way to suppress the thermal processes. But what can be done without cooling?

There are a few possibilities. One of them is to optimize the design of a detector to achieve the best performance at a given temperature and wavelength [6-8]. Optimization includes a careful selection of the semiconductor band gap and doping. Such a selection is possible with variable gap semiconductors, such as $\text{Hg}_{1-x}\text{Cd}_x\text{Te}$, $\text{Hg}_{1-x}\text{Mn}_x\text{Te}$ and $\text{Hg}_{1-x}\text{Zn}_x\text{Te}$. The use of a lightly doped *p*-type material is preferable, since the Auger generation rate is smaller in comparison with *n*-type material. Another possibility is to reduce the volume of active element for maximum responsivity to noise ratio. This can be done by immersing the detector to a high refraction lens [8-16] and optical resonant cavity [8, 17].

Recently, Elliot and other British workers [18-27] proposed to suppress the Auger processes by the use of stationary non-equilibrium depletion of semiconductor in charge carriers. This can be achieved using minority carrier phenomena at the

light-heavy or heterojunction contacts such as exclusion [18–22, 30] and extraction [22–28]. Another possibility is to use the magnetoconcentration effect [31–33].

To analyse the limitations of IR detector performance and possible ways to overcome the limitations, let us consider a simplified model of a photodetector as a slab of homogeneous semiconductor material with an actual electrical area A_e and thickness d (Fig. 1). The current responsivity of the device is

$$R_i = \Delta I / \Delta P_o \quad (1)$$

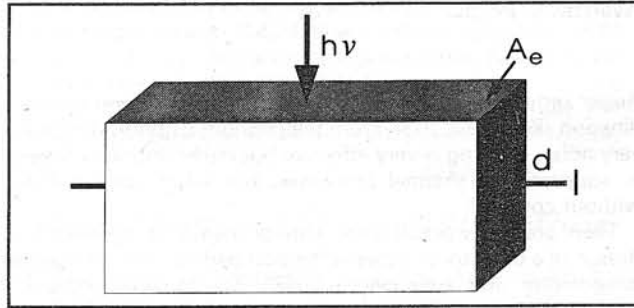


Fig. 1. The simplified model of photodetector

where ΔI is the increase of photocurrent due to the increase of optical power ΔP_o . The current responsivity is determined by quantum efficiency and by photoelectrical gain g . The quantum efficiency is the number of electron-hole pairs generated per incident photon. The photoelectrical gain is the number of carriers passing contacts per one generated pair. Both values are assumed to be constant over the active area. For monochromatic radiation the responsivity is

$$R_i = \frac{\lambda \eta}{hc} qg \quad (2)$$

where λ is the wavelength, h is the Planck constant, c is the light velocity and q is the electron charge.

The current passing contacts of the device is noisy due to statistical nature of the generation and recombination processes. The current noise is [1]

$$I_n^2 = 2(G + R) A_e \cdot d \cdot \Delta f \cdot q^2 \cdot g^2 \quad (3)$$

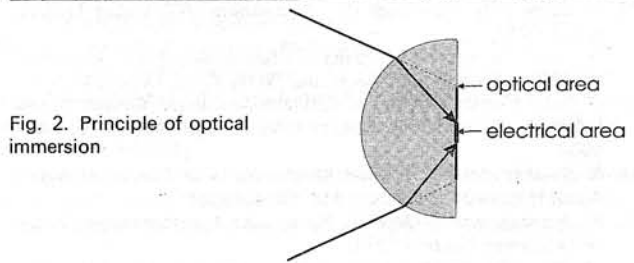


Fig. 2. Principle of optical immersion

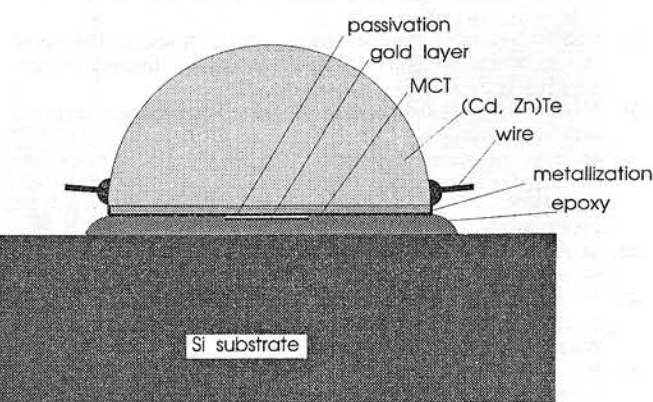


Fig. 3. Structure of monolithic optically immersed photoconductor

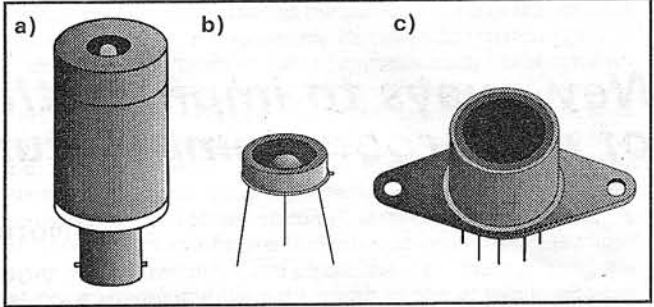


Fig. 4. Optically immersed ambient temperature (a, b) and two-stage thermoelectrically cooled (c) 10,6 μm photoconductors

Detectivity D^* is the main parameter characterizing normalized signal-to-noise performance of detectors.

$$D^* = R_i (A_o \Delta f)^{1/2} / I_n \quad (4)$$

According to Eqs. (2)–(4)

$$D^* = \frac{\lambda}{hc} \cdot \left(\frac{A_o}{A_e}\right)^{1/2} \cdot \frac{\eta}{d^{1/2}} \cdot [2(G + R)]^{1/2} \quad (5)$$

As the latter equation shows, the normalized detectivity at a given wavelength can be maximized if:

- the optical to electrical area ratio is high,
- the quantum efficiency to square root of thickness ratio is high,
- the sum of generation and recombination rate is low.

The detectivity would be proportional to the wavelength, provided that all material parameters are independent of wavelength, expressing the simple fact that the photon energy is inversely proportional to the wavelength.

The factor $(A_o/A_e)^{1/2}$ is the square root of the ratio of the optical to electrical area of the detector. In most detectors, both areas are equal. There are, however, ways to make the optical area substantially greater than the electrical one. The optical immersion of detectors to a hemispherical or hyperhemispherical lens of high refraction index is an example of a very effective way to increase the A_o/A_e ratio. Fig. 2 shows the principle of optical immersion. Due to immersion, the linear area of the detector increases by a factor of n or n^2 for hemispherical or hyperhemispherical immersion, respectively. As a result, the detectivity is increased by the same factor. Germanium ($n = 4$) is the most frequently used for the immersion lens [8–10]. The problems arising from difficulties in the mechanical matching of detector to the lens, transmission and reflection losses were solved by the use of monolithic technology developed recently at VIGO [12–14]. In this technology the immersion lens is formed directly in transparent CdZnTe substrate ($n = 2.7$) of epitaxial HgCdZnTe layers used as the sensitive element.

Fig. 3 schematically shows the structure of a monolithic, optically immersed photoconductor. Optical immersion offers the additional advantage of reducing bias power dissipation by factors of n^2 and n^4 in the case of hemi- and hyperhemispherical immersion, respectively. In the case of monolithic devices these factors are 7 and 49. Fig. 4 shows practical optically immersed 10.6 μm photoconductor manufactured by VIGO. The monolithic approach permits simple and economical manufacturing, the devices are rugged, mechanically stable and they can operate in a very broad spectral band with minimized reflection and absorption losses.

As Fig. 5 shows, the performance of immersed devices has been highly improved compared to that of conventional, non-immersed devices operating under the same conditions. It should be noted, that, in contrast to the cryogenic cooling, the gain in performance due to optical immersion is achieved without sacrificing response time. For example, the response time of the 10.6 μm photoconductors is shorter than 1 ns and 10 ns for the uncooled and two-stage TE-cooled devices, respectively.

Optical immersion can also successfully be used for photoelectromagnetic, Demer effect and photodiode detectors [8]. In contrast to photoconductors, these devices do not require

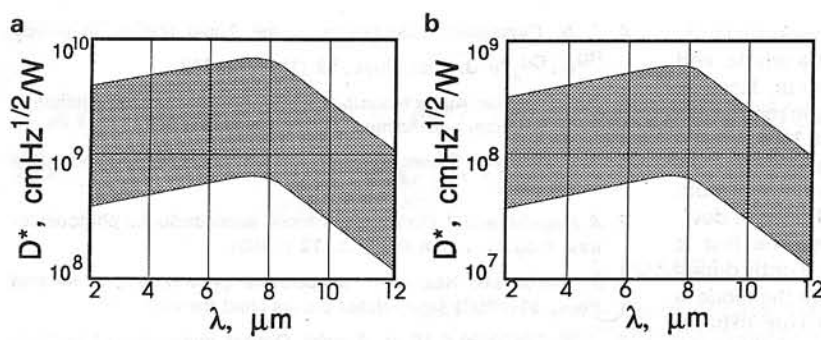


Fig. 5. Spectral detectivity of optically immersed ambient temperature (a) and two-stage thermoelectrically cooled (b) 10.6 μm photoconductors

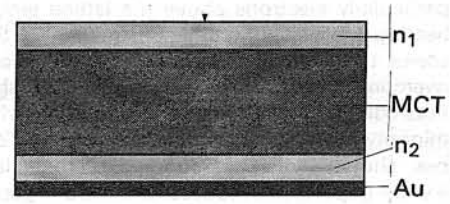


Fig. 6. Schematic structure of multilayer optical resonant cavity

biasing. They can operate effectively over a wide frequency band, starting from DC. This is due to the lack of low frequency noise and a very short time constant. The reduction of the electrical area size of the detector due to immersion has also additional advantages. The strong magnetic field required for a high quality photoelectromagnetic detector can be achieved much more easily. The capacity of the photodiode is reduced proportionally to the electrical area of the device.

Let us now return to the photodetector model and Eq. 5. Since the detectivity is proportional to the factor $\eta/d^{1/2}$, a high quantum efficiency must be achieved in thin devices. This is usually difficult to make, as the absorption of long-wave radiation in uncooled, narrow-gap semiconductors is weak. The quantum efficiency factor can be increased in devices with non-reflective frontside and highly reflective backside surfaces of the sensitive element. The effective absorption can be further improved by using the interference effect [6, 8, 17] to setup the resonant cavity. This can be achieved in a multilayer structure, shown in Fig. 6, in which the semiconductor flake is sandwiched between two dielectric layers and a metallic back reflecting mirror. The optimized resonant cavity structure with carefully selected thicknesses and reflection coefficients of all layers exhibit detectivity enhanced by a factor of about 2.5 at peak wavelength compared to optimized conventional device. It should be noted, that the interference effects strongly modify the spectral response of the device, and the optical cavity gain can be achieved only within narrow spectral regions.

As equation (5) shows, the generation and recombination rates should be minimized. At high temperature the thermal generation and recombination in $\text{Hg}_{1-x}\text{Cd}_x\text{Te}$ and other narrow-gap semiconductors with InSb-like band structure is

determined by the Auger-1 and Auger-7 processes [3-5]. The corresponding net generation rate (the difference between the generation and recombination rates) is [21]

$$G_A - R_A = \frac{n_i^2 - np}{2n_i^2} \left[\frac{n}{(1 + \alpha n)\tau_{A1}^i} + \frac{p}{\tau_{A7}^i} \right] \quad (6)$$

where τ_{A1}^i and τ_{A7}^i are the intrinsic Auger-1 and Auger-7 recombination times, n_i is the intrinsic concentration $\alpha^{-1} = 1.9 \cdot 10^{17} \text{ cm}^{-3}$.

As equation (6) shows, in the equilibrium state, the net Auger generation and recombination rates are equal. Both rates increased exponentially with temperature. Since τ_{A1}^i is by a factor of 2 to 10 shorter than τ_{A7}^i , the $G_A + R_A$ achieves its minimum in lightly doped p -type material. This is the reason, why p -type doping is preferable for equilibrium mode photodetectors operated at high temperature. British workers [18-29] proposed a new approach to reducing the photodetector cooling requirements, which is based on the non-equilibrium mode of operation. Their concept relies on the suppression of the Auger processes by decreasing the free carrier concentration below its equilibrium values. This can be achieved, for example, in a biased I - h or heterojunction contacts. An example of excluding contact photoconductor material is shown in Fig. 7. The positively biased contact is a highly doped n^+ or wide-gap material, while the photosensitive area is a near-intrinsic ν -type material. Such a contact does not inject minority holes but permits the majority electrons to flow out of the device. As a result, the hole concentration also falls, to maintain electrical neutrality in the region. Reduced concentration of electron and holes result in the suppression of the Auger processes.

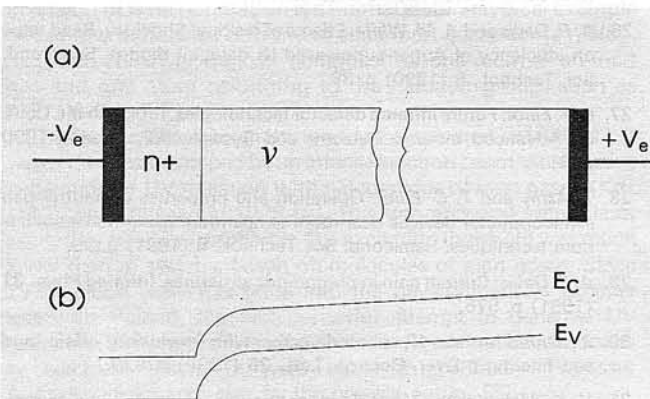
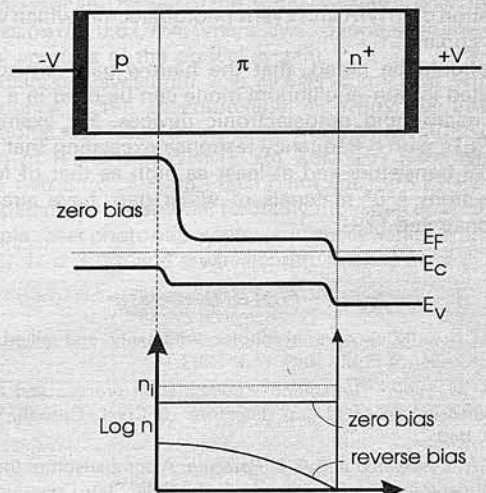


Fig. 7. Schematic structure of excluded contact photoconductor (a) and energy levels diagram (b)

Fig. 8. Schematic structure of extracted photodiode, showing energy levels and electron concentration



The electron field in the excluded region must be sufficiently low to avoid significant heating in the device as a whole, and particularly electrons above the lattice temperature. Electron heating is not an important constraint in the 3–5 μm region, but seems to restrict the usefulness of exclusion at 10.6 μm . To overcome the problem, the same British team proposed non-equilibrium photodiode structures, which employ both minority carrier exclusion and extraction [22–29]. These devices, shown in Fig. 8, consists of three layers. The first is a wide-gap n or n^+ , the second is narrow-gap and lightly doped π -type, and the third is a wide-gap p or p^+ . When the diode is reverse biased, the junction between π and n -type extracts electrons, which cannot be replenished by the excluding $p^+ \pi$ contact so the electron density drops by several orders of magnitude throughout the π region. The hole concentration also falls to keep space charge neutrality. This results in suppression of Auger processes and in noise reduction.

The non-equilibrium structures only can be handled by numerical methods, since the usual approximations break down. Such features as degeneracy, non-parabolicity, compensation, large deviation from equilibrium state, various generation-recombination mechanisms and graded interfaces should also be taken into account. The calculations show, that the extracted photodiodes have a potential for BLIP operation in the 8–14 μm band at temperature of about 230 K, which is achievable with simple two-stage thermoelectrical coolers.

Another method to obtain stationary non-equilibrium depletion of the semiconductor is to use the magnetoconcentration effect [31–33]. The depletion in the device is achieved due to the Lorentz force which deflects both electron and hole towards the backside surface of the high surface recombination. As a result, most of the semiconductor becomes highly depleted.

Excluded photoconductors [19, 21, 24, 26–29], extracted photodiodes [26–27], and magnetoconcentration devices [30–32] have been demonstrated in practice. Significant reduction of leakage currents have been achieved. The improvement of performance was relatively modest. Problem arise from excessive currents due to Shockley-Read generation and due to flicker noise.

The BLIP limit can be achieved by the use of extremely high quality materials, with controlled doping at very low levels ($< 10^{13} \text{ cm}^{-3}$) and with a very low concentration of Shockley-Read centers. Utmost care must also be taken with contact and passivation technology. In this respect, the heterostructure passivations and contacts are strategically important. The achievement of potential performance of the non-equilibrium devices in practice would require well-established epitaxial technology, which is not yet sufficiently developed.

The conditions for BLIP limit can be significantly softened, however, by the combination of Auger suppression with optical immersion. The reduction of bias power dissipation due to optical immersion is also extremely important for two-dimensional arrays. The resulting devices show great promise for BLIP operation of MWIR and LWIR photodetectors which would not need cooling.

It should be noted, that the narrow-gap semiconductors operated in non-equilibrium mode can be used in a variety of new micro- and optoelectronic devices. For example, InSb MISFETs with a frequency response exceeding that of silicon NMOS transistors and at least as high as that of MODFETs made from A^3B^5 materials of wider gap, have already been demonstrated [29].

References

1. A. Rose: Concepts of photoconductivity and allied problems. Interscience Publ., New York 1963.
2. A. M. White: Generation-recombination process and Auger suppression in small-gap detectors. *J. Cryst. Growth*, **66** (1988) p. 840.
3. T. N. Casselman and P. E. Petersen: A comparison of the dominant Auger transitions in p-type HgCdTe. *Solid State Commun.*, **3** (1980) p. 615.

4. T. N. Casselman: Calculations of the Auger lifetime in p-type $\text{Hg}_{1-x}\text{Cd}_x\text{Te}$. *J. Appl. Phys.*, **52** (1981) p. 848.
5. P. E. Petersen: Auger recombination in mercury cadmium telluride. *Semiconductor and Semimetals*, **18** (1981) p. 121.
6. D. L. Spears: in "Proc. IRIS Specialty Group on IR Detectors", San Diego 1982.
7. A. Rogalski and J. Piotrowski: Intrinsic semiconductor photodetectors. *Prog. Quantum Electron.*, **12** (1988).
8. J. Piotrowski: Near-room temperature photodetectors. *Infrared Phys.*, **31** (1990) (and related papers cited therein).
9. J. E. Slavek and H. H. Randa: Optical immersion of HgCdTe photoconductive detectors. *Infrared Phys.*, **15** (1975) p. 339.
10. I. C. Carmichael: Optical immersion of a cryogenically cooled 77 K photoconductive CdHgTe detector. In "Advances Infrared Detectors and Systems", IEE, London 1983 p. 45.
11. T. Piganeau: Optical immersed type photovoltaic detector. *Us Patent* 4, 638, 828 (1987).
12. M. Grudzień: Patent application.
13. M. Grudzień and J. Piotrowski: Monolithic optically immersed HgCdTe IR detectors. *Infrared Phys.*, **29** (1989) p. 251.
14. VIGO Data Sheets, Warsaw 1992.
15. N. T. Gordon: Design of HgCdTe infrared detector arrays using immersion with microlens to achieve a higher operating temperature. *Semicond. Sci. Technol.*, **8** (1991) p. 106.
16. C. L. Jones et al.: Fabrication and assessment of optically immersed CdHgTe detector arrays. *Semicond. Sci. Technol.*, **8** (1991) p. 110.
17. D. L. Spears: 10.6 micron photomixer arrays at 195. In "Proc. of IRIS Active Systems", 1984 p. 331.
18. C. T. Elliot: Cadmium mercury telluride infrared detectors. *J. Cryst. Growth*, **72** (1985) p. 453.
19. T. Ashly and C. T. Elliot: Non-equilibrium mode of operation for infrared detection. *Electron. Lett.*, **21** (1985) p. 451.
20. T. Ashly: Non-equilibrium devices for infrared detection. *Proc. SPIE*, **572** (1985) p. 123.
21. A. M. White: The characteristics of minority-carrier exclusion in narrow direct gap semiconductors. *Infrared Phys.*, **25** (1985) p. 729.
22. T. Ashly: Non-equilibrium mode of operation for infrared detection. *Infrared Phys.*, **26** (1986) p. 303.
23. A. M. White: Auger suppression and negative resistance in low gap diode structures. *Infrared Phys.*, **26** (1986) p. 317.
24. A. M. White: Negative resistance with Auger suppression in near-intrinsic low-band gap photo-diode structure. *Infrared Phys.*, **27** (1987) p. 361.
25. C. T. Elliot: Non-equilibrium mode of operation of narrow-gap semiconductor devices. *Semicond. Sci. Technol.*, **5** (1990) p. 30 (and other related papers cited therein).
26. A. P. Davis and A. M. White: Effects of residual Shockley-Read traps on efficiency of Auger-suppressed IR detector diodes. *Semicond. Sci. Technol.*, **5** (1990) p. 38.
27. C. T. Elliot: Future infrared detector technologies. *Proc. 4th Int. Conf. on Advanced Infrared Detector and Systems*, IEE, London 1990 p. 61.
28. T. Ashly and T. C. Elliot: Operation and properties of narrow-gap semiconductor devices near room temperature using non-equilibrium techniques. *Semicond. Sci. Technol.*, **8** (1991) p. 99.
29. A. P. Davis: Current gain in photodiode structures. *Infrared Phys.*, **31** (1991) p. 575.
30. Z. Djuric et al.: IR photodetector with exclusion effect and self-filtering n layer. *Electron. Lett.*, **26** (1990) p. 929.
31. V. K. Malyutenko: Magnetoconcentration effect at Auger recombination of current carriers. *Phys. Status Solidi A*, **65** (1981) p. 131.
32. Z. Djuric and J. Piotrowski: Room temperature IR photodetector with electromagnetic carrier depletion. *Electron. Lett.*, **26** (1990) p. 1689.
33. Z. Djuric and J. Piotrowski: Electromagnetically carrier depleted infrared photodetector. *Proc. SPIE*, **1540** (1992) p. 1540.